Trajectory Optimization Strategies for the Simulation of the ADS-33 Mission Task Elements*

C.L. Bottasso†, **F. Scorcelletti**‡, **G. Maisano**§, **A. Ragazzi**¶

Politecnico di Milano

Milano, Italy

Abstract

This paper is concerned with the formulation of ADS-33 Mission Task Elements (MTEs) as trajectory optimization problems, and describes efficient numerical solution procedures for this class of problems. MTEs are maneuvers specifically designed to quantify the Handling Qualities of rotorcraft vehicles. Here we show that MTEs, being characterized by a mission target which must be accomplished while satisfying a set of constraints, can be readily described in a precise mathematical sense by defining equivalent constrained optimal control problems, whose solution yields the best possible performance of a given helicopter in performing a given MTE. The capabilities of the proposed methodology are demonstrated with the help of representative numerical simulations.

1 INTRODUCTION

This paper is concerned with the application of trajectory optimization procedures to the simulation of ADS-33 Mission Task Elements (MTEs) [1] using flight mechanics models of rotorcraft vehicles. Flight mechanics models are typically used for the characterization of equilibria, the so-called trim states, and for dynamic response simulations, i.e. the evaluation of the vehicle state time histories for given initial conditions and given control inputs. For such purposes, several general codes are available and widely used by industry, as for example CAMRAD/JA [2], EUROPA [3], FLIGHTLAB [4], GenHel [5], etc.

In this paper a more general and complex simulation scenario is considered. The term *trajectory optimization* refers to the process of computing the optimal control inputs and the resulting response of a model of a vehicle, a rotorcraft in the present case, which minimize a cost function (or maximize an index of performance) while satisfying given constraints (which specify, for example, the vehicle flight envelope boundaries, and/or safety and procedural requirements for a

* Paper presented at the European Rotorcraft Forum, September 16–19, 2008, Arena and Convention Centre, Liverpool, UK.

† Associate Professor, e-mail: carlo.bottasso@polimi.it.

‡ Ph.D. candidate, AgustaWestland flight mechanics engineer.

§ Ph.D. candidate.

¶ AgustaWestland flight mechanics specialist.

maneuver of interest). We remark that this problem differs significantly from the usual and more common problem of *forward simulation* starting from given initial conditions under the action of control inputs, both in the case when the control time histories are given a priori or when they are computed by a flight control system or tracking controller. In fact, in order to use a typical forward simulation code, one has to specify a time history of control inputs, or a trajectory or sequence of trim conditions that the vehicle should track. In a trajectory optimization problem none of these two pieces of information, controls or trajectory, are known; in fact, both control inputs and trajectory are unknown and must be computed by solving an appropriate optimal control problem.

Many problems in vehicle dynamics can be studied with the help of trajectory optimization. In the area of rotorcraft flight mechanics, we mention here continued and rejected take-off procedures following an engine failure (Category A certification [6]), optimal auto-rotation, landing procedures after tail-rotor loss, approach and departure from flight decks, and of course the definition of ADS-33 MTEs [1], which are the subject of the present work.

Trajectory optimization codes implement appropriate numerical methods which, interacting with forward simulators, augment their capabilities in order to compute the controls which fly the vehicle model in an optimal and constraint-satisfycing way. Computer implementations of trajectory optimization procedures for rotorcraft flight mechanics vehicle models have been previously described by Okuno and Kawachi [7], Carlson and Zhao [8], and Bottasso et al. [9, 10, 11]. The extension of such procedures to handle fine-scale aero-servo-elastic comprehensive vehicle models have been first described by Bottasso et al. [12, 13, 11].

In the present work, we use the Trajectory Optimization Program (TOP), developed at the Department of Aerospace Engineering of the Politecnico di Milano. TOP has been designed to solve efficiently trajectory optimization problems for rotorcraft vehicles, and has some unique features, including multiple solution algorithms which are tuned and optimized to the level of complexity of the vehicle model. In this paper, we use flight mechanics models of low/moderate complexity, for which the preferred solution algorithm in TOP is a method termed Direct Transcription.

The paper is organized according to the following plan. At first an introduction to the ADS-33 MTEs is presented. Some basic elements on optimization and, specifically, the formulation of maneuvers as optimal control problems are given next. The paper continues discussing the Direct Transcription method used in this work for numerically solving trajectory optimization problems. Finally, we demonstrate the simulation of a selection of ADS-33 MTEs using the TOP software.

2 ADS-33 MISSION TASK ELEMENTS

The ADS-33 specification [1] defines a series of MTEs, which are precisely defined flight test maneuvers whose primary goals are the quantification of a rotorcraft ability to perform certain critical tasks and to provide a basis for an overall assessment of the specific level of Handling Qualities (HQ). Each MTE should be assessed by at least three pilots, who assign a subjective rate according to the Cooper-Harper-Rating Scale [1] through the definition of numerical values for Desired and Adequate performance. To allow for different standards of precision, the performance standards for each task are listed separately for different rotorcraft categories and for both Good Visual Environment (GVE) and Degraded Visual Conditions (DVE).

Analytical (i.e. non-piloted) simulations can be useful for predicting the ability of a rotorcraft to perform each MTE, identify potential adverse effects (e.g. high rotor and transmission loads), and determine whether the flight control laws are satisfactory. Extensive analytical simulations of MTEs can be performed inexpensively and with no risk. Therefore, they can complement piloted simulations and flight tests, and they can also be used during design to predict the HQ of a vehicle before a prototype is available.

Goal of this paper is to show that a general MTE simulation environment can be readily developed using trajectory optimization. In fact, the ADS-33 specification does not assign a-priori reference trajectories for the various MTEs, so that the classical inverse approach, consisting in finding the control time histories which fly the vehicle along a given trajectory, can not be easily used. Since a reference trajectory is not given, but rather each maneuver is defined by certain criteria and constraints, a more general simulation framework must be adopted.

Using the trajectory optimization approach, one has to translate the specification of each MTE into an appropriate optimal control problem. Path and flight envelope limits may be imposed by prescribing suitable constraints on the vehicle states and control inputs. Furthermore, the aggressiveness of the maneuver can be properly tuned by the specification of an appropriate cost function. A practical approach is to define the cost as the sum of two terms which are represented by an aggressiveness parameter (e.g., the maneuver duration as in the present work) and by a term which accounts for the piloting "effort" (e.g., the integral of the control rates, as in this paper). By weighting the relative importance of these two antithetic terms, it is possible to increase the maneuver aggressiveness until one or more flight envelope limits (i.e. actuator saturation, load factor, etc.) are reached. More details about this point and specifically about the choice of the merit function are discussed in §5.1.

3 FORMULATION OF MANEUVERS AS OPTIMAL CONTROL PROBLEMS

A maneuver can be defined as a finite-time transition between two trim conditions [14]*. Clearly, given a starting trim and an arrival trim, there is an infinite number of ways to transition between the two. A way to remove this arbitrariness is to formulate a maneuver as an optimal control problem [10, 12, 11], where one minimizes a cost (time, altitude loss, control activity, fuel consumption, etc.) which in general is some given function of the vehicle states and control inputs. The solution of the optimization problem must satisfy the dynamic and kinematic equations of the vehicle, the initial and final conditions corresponding to the start and arrival trims, and all other equality and inequality constraints which need to be met in order to satisfy given performance and procedural requirements.

Consider a flight mechanics vehicle model $\mathcal{M}$, which includes structural and aerodynamic models of the vehicle components, possibly (but not necessarily) using a multibody approach [15]. The dynamics of model $\mathcal{M}$ can in general be described in terms of a set of non-linear differential

* Although this is the only rigorous definition of a maneuver, in the context of the present work it will be more useful to use the term maneuver more loosely, and in general we can consider also the case of terminal conditions which are not trimmed.

algebraic equations written as

$$\boldsymbol{f}_{\mathrm{SD}}(\dot{\boldsymbol{x}}_{\mathrm{SD}}, \boldsymbol{x}_{\mathrm{SD}}, \boldsymbol{\lambda}, \boldsymbol{x}_{\mathrm{A}}, \boldsymbol{u}) = 0, \tag{1a}$$

$$\boldsymbol{c}(\boldsymbol{x}_{\mathrm{SD}}) = 0, \tag{1b}$$

$$\boldsymbol{M}\dot{\boldsymbol{x}}_{\mathrm{A}} + \boldsymbol{L}\boldsymbol{x}_{\mathrm{A}} - \boldsymbol{\tau}(\boldsymbol{x}_{\mathrm{SD}}, \boldsymbol{u}) = 0, \tag{1c}$$

where $\boldsymbol{x}_{\mathrm{SD}}$ are the structural dynamics states (including states which describe rigid and possibly flexible rotor(s), fuselage, engine, etc.), $\boldsymbol{\lambda}$ are constraint-enforcing Lagrange multipliers in a multibody vehicle model, $\boldsymbol{x}_{\mathrm{A}}$ are aerodynamic states (e.g. dynamic inflow variables), and $\boldsymbol{u}$ is the control input vector. Equations (1a) group together the equations of dynamic equilibrium and the kinematic equations. Equations (1b) represent mechanical joint constraint equations in a multibody vehicle model, while Eqs. (1c) are the aerodynamic state equations. Finally, the notation $\dot{(\cdot)} = \mathrm{d}(\cdot)/\mathrm{d}t$ indicates a derivative with respect to time t.

For the sake of simplicity, in the following we will consider that the Lagrange multipliers $\boldsymbol{\lambda}$ and redundant structural dynamics states can always be formally eliminated in favor of a minimal set of coordinates [16]. The interested reader can refer to Ref. [17] for a description of the solution of optimal control problems for multibody models in redundant form; while this does not pose technical difficulties, it requires a heavier notation and complicates the discussion. Therefore, the governing equations will be assumed to be of the ordinary differential type and will be simply expressed as

$$\boldsymbol{f}_{\mathrm{SD}}(\dot{\boldsymbol{x}}_{\mathrm{SD}}, \boldsymbol{x}_{\mathrm{SD}}, \boldsymbol{x}_{\mathrm{A}}, \boldsymbol{u}) = 0, \tag{2a}$$

$$\boldsymbol{M}\dot{\boldsymbol{x}}_{\mathrm{A}} + \boldsymbol{L}\boldsymbol{x}_{\mathrm{A}} - \boldsymbol{\tau}(\boldsymbol{x}_{\mathrm{SD}}, \boldsymbol{u}) = 0. \tag{2b}$$

When using quasi-steady aerodynamics, the aerodynamic model expressed by Eq. (2b) and its associated aerodynamic states $\boldsymbol{x}_{\mathrm{A}}$ are of an algebraic nature. The numerical solution is in that case performed by eliminating the algebraic aerodynamic variables, usually through a fixed point iteration. Therefore, even in that case, we can consider an ODE model with no loss of generality.

It will be convenient to use a more synthetical form of the above equations in the following pages, and hence we will write the vehicle model as

$$\boldsymbol{f}(\dot{\boldsymbol{x}}, \boldsymbol{x}, \boldsymbol{u}) = 0, \tag{3a}$$

$$\boldsymbol{y} = \boldsymbol{h}(\boldsymbol{x}), \tag{3b}$$

where $\boldsymbol{x} = (\boldsymbol{x}_{\mathrm{SD}}^T, \boldsymbol{x}_{\mathrm{A}}^T)^T$ is the global state vector and $\boldsymbol{f}$ stacks together Eqs. (2a) and (2b). In addition, Eq. (3b) defines a vector of outputs $\boldsymbol{y}$. The outputs will typically represent some global vehicle states which describe its gross motion, such as position, orientation, linear and angular velocity of a vehicle-embedded frame with respect to an inertial frame of reference, or other quantities useful for formulating the maneuver optimal control problem.

Equations (3a) are solved for the forward simulation problem by providing a time history of control inputs $\boldsymbol{u}(t)$ and initial conditions on the states $\boldsymbol{x}(0) = \boldsymbol{x}_0$. Accordingly, one obtains also the associated values of the outputs through (3b).

The trajectory optimization problem is defined on the interval $\Omega = [0, T]$, $t \in \Omega$, where the final time T is typically unknown and must be determined as part of the solution to the problem.

Specific events might be associated with unknown time instants T_i, $0 < T_i < T$, as for example the reaching of specific values of certain states, the jettisoning of part of the cargo, etc. The present code implementation can handle multiple internal events, but we do not consider this case in the following for the sake of simplicity, since this does not pose any conceptual difficulty that is worth addressing in detail.

The maneuver optimization problem consists in finding the control function $\boldsymbol{u}(t)$, and hence through (3) the associated function $\boldsymbol{x}(t)$ and $\boldsymbol{y}(t)$, which minimize the general cost

$$J = \phi(\boldsymbol{y}, t)\Big|_0^T + \int_0^T L(\boldsymbol{y}, \boldsymbol{u}, \dot{\boldsymbol{u}}, t)\, \mathrm{d}t. \tag{4}$$

The first term in the previous expression is a boundary term which accounts for values of the outputs at the initial and/or final instants, while the second term is an integral cost term.

The minimizing solution must satisfy the vehicle equations of motion (3), together with the boundary (initial and/or terminal) conditions on the states

$$\boldsymbol{g}_{\mathrm{bc}}\big(\boldsymbol{x}(0)\big) \in [\boldsymbol{g}_{\mathrm{bc},0}^{\min}, \boldsymbol{g}_{\mathrm{bc},0}^{\max}], \tag{5a}$$

$$\boldsymbol{g}_{\mathrm{bc}}\big(\boldsymbol{x}(T)\big) \in [\boldsymbol{g}_{\mathrm{bc},T}^{\min}, \boldsymbol{g}_{\mathrm{bc},T}^{\max}]. \tag{5b}$$

Notice that the initial and final values of the states $\boldsymbol{x}(0)$ and $\boldsymbol{x}(T)$ are typically determined by solving a separate trim problem off-line, whose details depend on the specifics of the vehicle model being considered. Often, the final conditions are not required to represent a trim state, in which case the exit conditions can be written in terms of the sole outputs as

$$\boldsymbol{g}_{\mathrm{bc}}\big(\boldsymbol{y}(T)\big) \in [\boldsymbol{g}_{\mathrm{bc},T}^{\min}, \boldsymbol{g}_{\mathrm{bc},T}^{\max}]. \tag{6}$$

Other maneuver-defining and/or envelope-protection constraints can be expressed as generic algebraic non-linear constraints of the form

$$\boldsymbol{g}_{\mathrm{gen}}(\boldsymbol{y}, \boldsymbol{u}, t) \in [\boldsymbol{g}_{\mathrm{gen}}^{\min}, \boldsymbol{g}_{\mathrm{gen}}^{\max}], \tag{7}$$

integral conditions

$$\frac{1}{T}\int_0^T \boldsymbol{g}_{\mathrm{int}}(\boldsymbol{y}, \boldsymbol{u}, t)\, \mathrm{d}t \in [\boldsymbol{g}_{\mathrm{int}}^{\min}, \boldsymbol{g}_{\mathrm{int}}^{\max}], \tag{8}$$

constraints at unknown internal events T_i

$$\boldsymbol{g}_{\mathrm{event}}(\boldsymbol{y}, \boldsymbol{u}, T_i) \in [\boldsymbol{g}_{\mathrm{event}}^{\min}, \boldsymbol{g}_{\mathrm{event}}^{\max}], \tag{9}$$

or simple bounds

$$\boldsymbol{y} \in [\boldsymbol{y}^{\min}, \boldsymbol{y}^{\max}], \tag{10a}$$

$$\boldsymbol{u} \in [\boldsymbol{u}^{\min}, \boldsymbol{u}^{\max}]. \tag{10b}$$

In summary, the maneuver optimal control problem can be expressed as

$$\min_{\boldsymbol{x},\boldsymbol{y},\boldsymbol{u},T} \quad \text{Cost } J, \text{ Eq. (4)}, \tag{11a}$$

$$\text{s.t.:} \quad \text{ODE system (3)}, \tag{11b}$$

$$\text{Constraints (5–10)}. \tag{11c}$$

4 DIRECT SOLUTION OF TRAJECTORY OPTIMIZATION PROBLEMS

The indirect approach to the solution of the maneuver optimal control problem (11) amounts to augmenting the cost (4), by adjoining the governing equations (3) with a set of co-states, and adjoining all other constraints conditions (5–10) with Lagrange multipliers. By imposing the stationarity of the augmented cost, one derives a new set of equations with their associated boundary conditions, which govern the optimal control problem [18]. The resulting boundary value problem can then be discretized using a suitable numerical method defined on a computational grid. This transforms the infinite dimensional boundary value problem into a discrete problem, whose unknowns are the values of the variables (states, co-states, Lagrange multipliers, controls) on the computational grid.

It is clear that the implementation of this classical approach requires the manipulation of the governing Eqs. (3) in order to derive the optimal control equations. This is a non-trivial task for complex and highly non-linear models, which might necessitate the use of symbolic manipulation or automatic differentiation tools to be carried out effectively. More importantly, this approach must be ruled out whenever one does not have access to the analytical expression of Eqs. (3) or their software implementation, as it is the case whenever the flight simulator is a third-party black-box code.

To overcome these limitations of the indirect approach, one can use the direct method [19]. In this case, instead of first optimizing and then discretizing, one first discretizes the model Eqs. (3) through a numerical method. This has the effect of discretizing also the cost function (4) and the constraints (5–10). This in turn defines a discrete parameter optimization or non-linear programming (NLP) problem [20], which can be written in general as

$$\min_{\boldsymbol{z}} \quad K(\boldsymbol{z}), \tag{12a}$$

$$\text{s.t.} \quad \boldsymbol{a}(\boldsymbol{z}) = \boldsymbol{0}, \tag{12b}$$

$$\boldsymbol{b}(\boldsymbol{z}) \in [\boldsymbol{b}^{\min}, \boldsymbol{b}^{\max}], \tag{12c}$$

where $\boldsymbol{z}$ is a set of algebraic unknowns, and K is a scalar objective function which represents an approximation of the cost J of Eq. (11a). The equality constraints (12b) are generated by the discretization of the equations of motion (11b), while the inequality constraints (12c) by all maneuver-defining constraints (11c). The specific form of the vector of algebraic unknowns and of the constraints depends on the method used for performing the discretization.

Necessary conditions for a constrained optimum for problem (12) are obtained, similarly to the optimal control case, by combining the objective K with the constraints through the use of Lagrange multipliers, and imposing the stationarity of the augmented objective function. By using the direct approach, one does not need to manipulate the equations of motion of the vehicle, since all that is required is the evaluation of the discretized equations on a step or sequence of steps, and this enables the interfacing to black-box vehicle simulators. For further possible advantages of the direct method, the interested reader is referred to Ref. [19].

We have found that, for the problems considered here, it is important for robustness to consider a scaled version of the NLP problem, where the NLP variable $\boldsymbol{z}$ is replaced by a scaled variable $\bar{\boldsymbol{z}} = \text{diag}(\boldsymbol{w}_z)\boldsymbol{z}$, $\boldsymbol{w}_z$ being a vector of scaling coefficients chosen so that the new unknown is $\bar{\boldsymbol{z}} \approx \mathcal{O}(\boldsymbol{1})$. Furthermore, since at convergence many constraints are active (at least all of the equality constraints (12b)), we have found that faster convergence of the SQP solver is obtained by using a slightly looser tolerance for the equality constraint feasibility than for the solution optimality tolerances. This in fact has the effect of avoiding repeated changes in the active set when trying to satisfy optimality at the end of the process, which eases the reaching of the exit condition of the NLP solver with basically no effect on the solution accuracy.

In the next section the direct method considered in this work is described in details; our numerical approach leads to sparse NLP problems (12), which in the present implementation are solved using sequential quadratic programming (SQP) [21].

4.1 Direct Transcription

We consider the partition of the time interval Ω as $0 = t_0 < t_1 < \ldots < t_N = T$, where the generic time element is $\Omega^n = [t_n, t_{n+1}]$, $n = (0, N-1)$, of time step size $h^n = t_{n+1} - t_n$. Here and in the following, quantities associated with the generic element vertex j are indicated using the notation $(\cdot)_j$, while quantities associated with the generic element k are labeled $(\cdot)^k$. Clearly, $h^n = h^n(T)$, i.e. the time step size is a function of the final time, when T is unknown.

In each time element Ω^n, the governing Eqs. (3a) are discretized using a suitable numerical method. The resulting discrete equations are expressed here as

$$\boldsymbol{f}_h(\boldsymbol{x}_{n+1}, \boldsymbol{x}_n, \boldsymbol{u}^n, h^n) = 0, \qquad n = (0, N-1), \tag{13}$$

where $\boldsymbol{f}_h$ is an algorithmic approximation of function $\boldsymbol{f}$ of Eq. (3a), $\boldsymbol{x}_n$, $\boldsymbol{x}_{n+1}$ are the values of the state vector at t_n and t_{n+1}, respectively, while $\boldsymbol{u}^n$ represents the value of the control vector within the step. In general there might be additional internal stages for both the state and the control variables, depending on the numerical method. For notational simplicity we do not consider that case here. With respect to this point, note further that in the case of higher order schemes with internal stages, Eqs. (13) might have been obtained by static elimination of these stages at the element level.

In the Direct Transcription case, the NLP problem (12) is defined as follows. First, the NLP variable is chosen as:

$$\boldsymbol{z} = (\boldsymbol{x}_{n=(0,N)}, \boldsymbol{u}^{n=(0,N-1)}, T)^T, \tag{14}$$

i.e. it is composed of the discrete states and control values on the computational grid, and the final time. Next, the cost J of Eq. (4) is discretized in terms of $\boldsymbol{z}$ as given by (14), obtaining the discrete cost K of Eq. (12a). Then, the discretized ODEs within each step, Eqs. (13), become the set of NLP equality constraints appearing in Eq. (12b). Finally, all other problem constraints and bounds, Eqs. (5–10), are expressed in terms of the NLP variables $\boldsymbol{z}$ and become the NLP inequality constraints of Eq. (12b).

The optimality conditions of the resulting discrete NLP problem converge to the optimality conditions of the optimal control problem (11) as the grid is refined and the number of discrete optimization variables goes to infinity [22].

The resulting problem is large but very sparse. In TOP, when using the internal flight mechanics model, the NLP problem Jacobian is evaluated using automatic differentiation with the ADOL-C code [23]. In the case of the black-box models (e.g. FLIGHTLAB and EUROPA), the Jacobian is obtained by sparse finite differencing.

5 NUMERICAL APPLICATIONS

In this section we present a few numerical applications of the methods described in the previous pages. Initially we introduce a test case which consists in a simple maneuver, for the purpose of explaining the MTE simulation approach adopted in the present work. Next, three ADS-33 MTEs are discussed and numerical results are presented.

All examples reported here use a FLIGHTLAB [4] helicopter model of a generic medium-size multi-engine four-bladed utility vehicle in the 9 ton class. The numerical model is based on three-dimensional rigid body dynamics, where rotor forces and moments are computed by using an actuator disk model with uniform inflow. Look-up tables are used for the quasi-steady aerodynamic coefficients of the vehicle lifting surfaces. A ground effect model is introduced in order to accurately reproduce the MTE flight tests. The controls are defined as $\boldsymbol{u} = (\theta_{0_{MR}}, \theta_{0_{TR}}, A_1, B_1)^T$, where $\theta_{0_{MR}}$ is the main rotor collective, $\theta_{0_{TR}}$ is the tail rotor collective, A_1, B_1 are the lateral and longitudinal cyclics, respectively.

For each MTE simulation, we refer to the Cargo/Utility in GVE performance standards as documented in Ref. [1].

5.1 Simulation Approach

As anticipated in Section 2, the MTE simulations are carried out by imposing the path constraints as inequality constraints according to Eqs. (5–10), and selecting the maneuver aggressiveness by the use of a cost function defined as follows:

$$J = T^2 + \frac{1}{\rho T} \int_0^T \dot{\boldsymbol{u}} \cdot \dot{\boldsymbol{u}} \, \mathrm{d}t. \tag{15}$$

The first term accounts for the aggressiveness of the piloting style, in this specific case the square of the total maneuver duration, while the second one is related to the integral of the control rates. The parameter ρ can be used to increase the maneuver aggressiveness, by increasing or decreasing the relative importance of the first and second terms of the cost.

A typical MTE simulation problem consists in evaluating a maneuver while satisfying certain constraints within a given time. The present approach guarantees that the path constraints are fulfilled, since these are included in the optimization constraints; furthermore, by tuning the aggressiveness parameter ρ, one has the ability to regulate the maneuver duration in order to be in compliance with the maximum time requirement. Clearly, there is a specific limit for the parameter ρ associated with the vehicle flight envelope constraints; when this limit is reached, the performance can not be increased further, since this would require violating one or more of the constraints, and the vehicle considered will have a certain level of Handling Qualities according to this limit condition.

In order to illustrate this simulation approach, consider the following example, consisting in a Depart maneuver [1]. The Helicopter is initially in Hover and is supposed to reach a steady Forward Flight condition at the speed of 50 Knots. The merit function is expressed by Eq. (15) and maneuvers are evaluated for three increasing values of the weight ρ; the simulations are performed using a uniform grid composed by 40 time steps. Typically for this kind of analyses the number of steps is chosen according to a convergence criteria: the grid is refined until the difference between two iterates (quantified by a specific measure) is smaller then a fixed tolerance. In Figure 1 (left), the pitch angle time histories are shown; the figure shows that, as the parameter ρ increases, the maneuver duration is reduced and the peak value of the pitch angle increases, since the maneuver is flown more aggressively. Figure 1 (right) reports the longitudinal cyclic. The different boundary values at $t = 0$ and $t = T$ are related to the different initial and final trim condition: Hover and Forward Flight at 50 Knots, respectively.

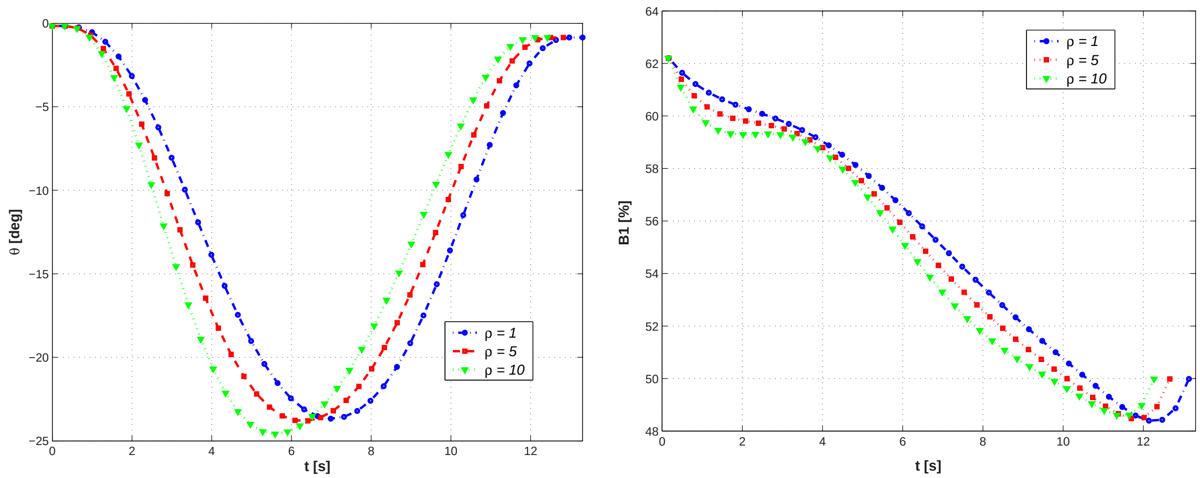

(a) *Pitch.* (b) *Longitudinal cyclic.*

Fig. 1: **Depart maneuver.**

5.2 Lateral Reposition

According to the Lateral Reposition MTE [1], the helicopter, initially in Hover, is supposed to translate laterally for 400 ft and then recover the initial Hover configuration. The maneuver must be flown in ground effect since the initial and final positions are characterized by an altitude of 35 ft (the rotor diameter is 30 ft); altitude variations must be within ±10 ft. Referring to Figure 2, the maximum allowed displacement in the longitudinal direction is ±10 ft, while the maximum heading misalignment is ±10 deg with respect to the initial direction. The maneuver must be completed within 18 seconds.

The trajectory constraints are imposed directly through bounds on the position variables and heading angle

$$|\psi(t)| < 10\text{deg}, \quad |x(t)| < 10\,\text{ft}, \quad |z(t)| < 10\,\text{ft}, \quad 0 \le y(t) \le 400\,\text{ft}. \tag{16}$$

It should be noted that the y-overshooting is avoided with this approach.

The minimum time problem, according to the merit function expressed by Eq. (15), was solved with an appropriate value of the aggressiveness parameter ρ, such that the maneuver duration is less than the maximum time allowed.

The numerical solution is obtained on a non-uniform computational grid of 80 time steps; a chebychev node distribution is introduced in order to improve the accuracy at the boundaries of the simulation domain.

Figure 3 shows some snapshots of the helicopter during the maneuver. Figure 4 shows the control time histories (in percentage of the variation range): the longitudinal and lateral cyclic inputs are characterized by high boundary rates which are accurately captured by the chebychev node distribution. Figure 5 reports the vehicle attitude time history in terms of its Euler angles. The maneuver duration is of about 14 s, less then the 18 s prescribed by the normative. Notice that the heading angle reaches its upper allowed bound during this maneuver; to account for model approximations, one could consider more conservative constraints than the ones prescribed by the specification.

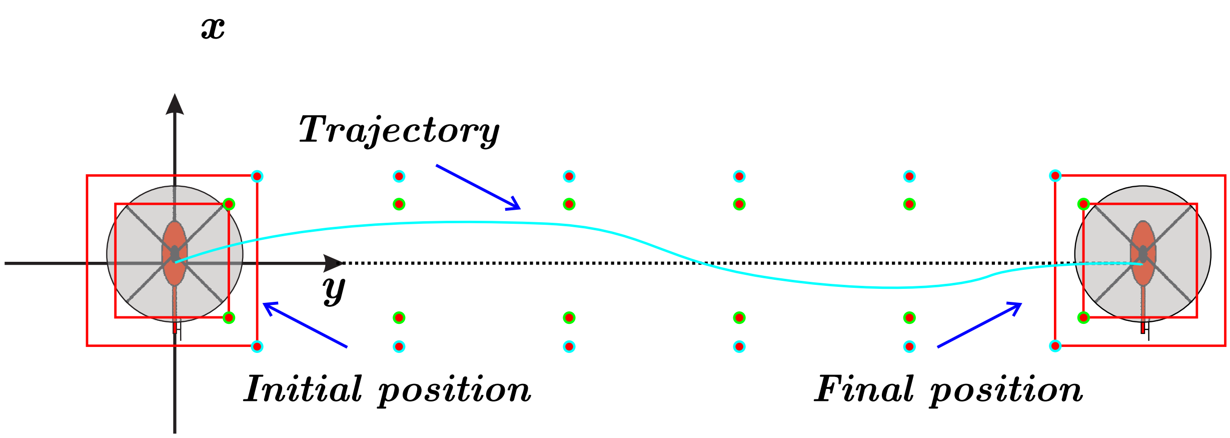

Fig. 2: **Lateral Reposition. Top view.**

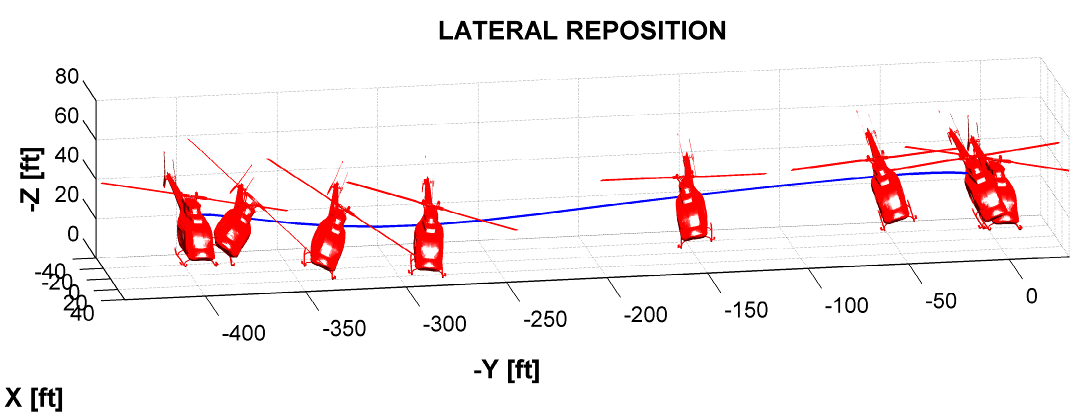

Fig. 3: **Lateral Reposition. Snapshots.**

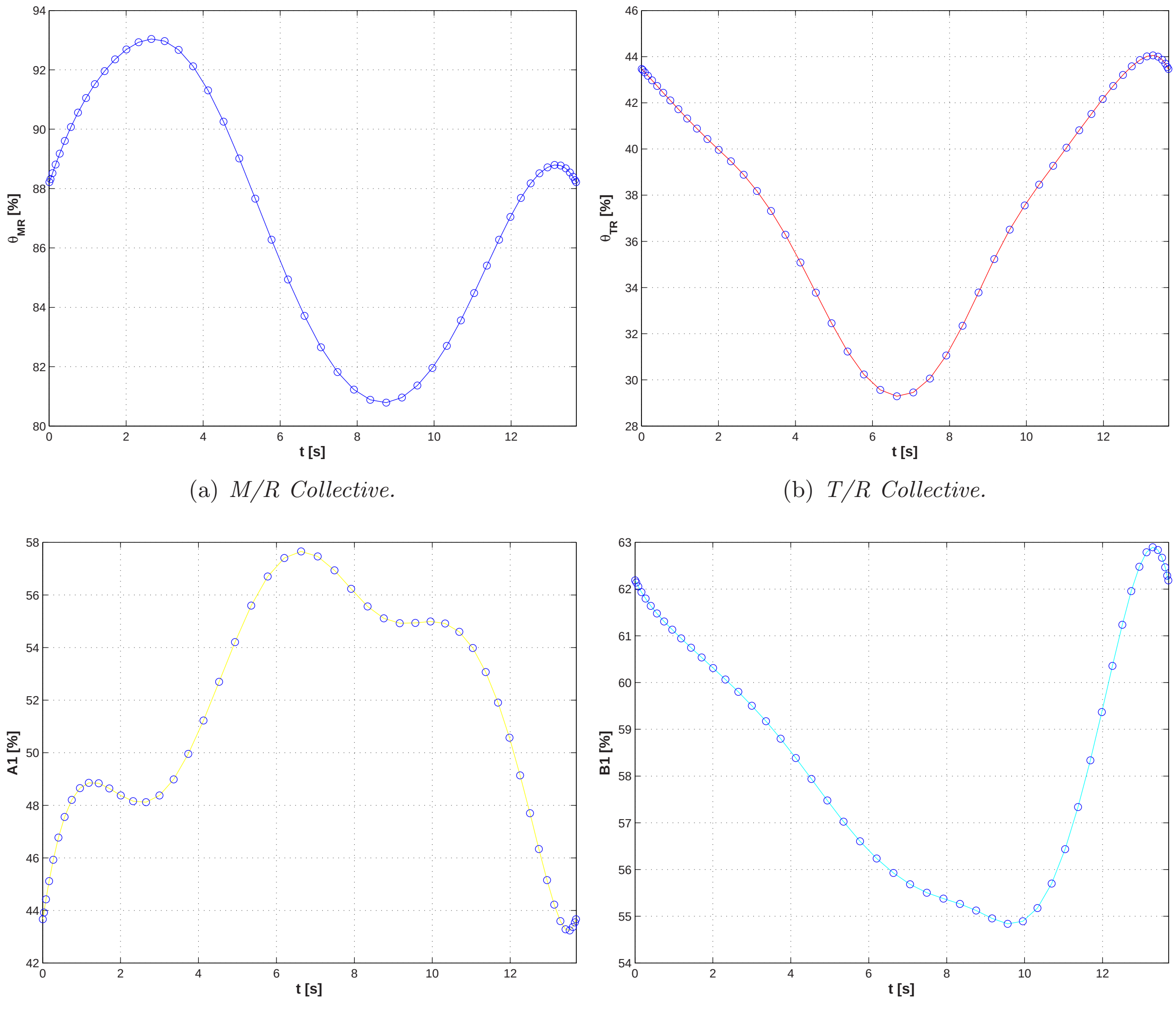

(a) *M/R Collective.*

(b) *T/R Collective.*

(c) *Lateral Cyclic.*

(d) *Longitudinal Cyclic.*

Fig. 4: **Lateral Reposition. Control inputs.**

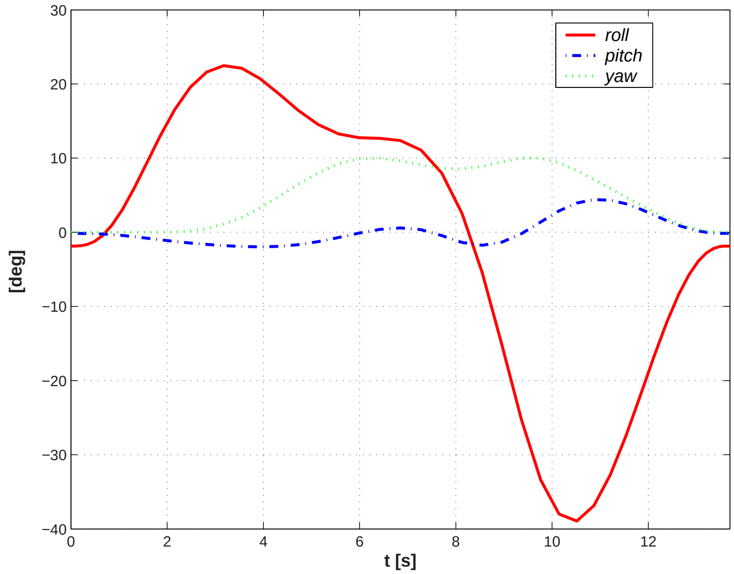

Fig. 5: **Lateral Reposition. Attitude angles.**

5.3 Pirouette

The Pirouette MTE is quite a complex maneuver; in fact the helicopter, starting from the Hover condition, must move along a circumference of radius $R = 100$ ft pointing its nose towards the center, and finally reaching the Hover state. As shown in Figure 6, there are constraints on the radial displacement, which must be less then ΔR ± 10 ft, and on the heading misalignment, $\Delta\psi$ ± 10 deg. Finally the maneuver must be accomplished within 45 s. Also in this case the maneuver is performed at an altitude of 10 ft (± 10 ft) so that ground effects are not negligible.

The typical execution of this maneuver can be divided in three phases. The first part is characterized by a transition from Hover to a steady turn in lateral flight. The opposite transition is accomplished at the end of the maneuver when the Hover state must be recovered. The cental part of the maneuver is characterized by a steady turn with an appropriate angular velocity. The simulation strategy reflects this subdivision, and it is effectively the result of two optimized maneuvers with a trim condition interposed between them. The first and last transitions are formulated in exactly the same manner, except for the boundary conditions which are inverted; for the internal phase a steady turn in lateral flight at the velocity of 11 Knots is assumed. Each transition is characterized by a chebychev grid of 50 time elements and, according to the ADS-33 specification, the following additional constraints are enforced at each grid node:

$$\left[\frac{r(t_i) - R}{\Delta R}\right]^2 \leq 1, \quad i = 0 \ldots N, \tag{17a}$$

$$\left[\frac{\psi(t_i) - \gamma(t_i)}{\Delta\psi}\right]^2 \leq 1, \quad i = 0 \ldots N, \tag{17b}$$

where $\gamma \triangleq tan^{-1}(y/x)$.

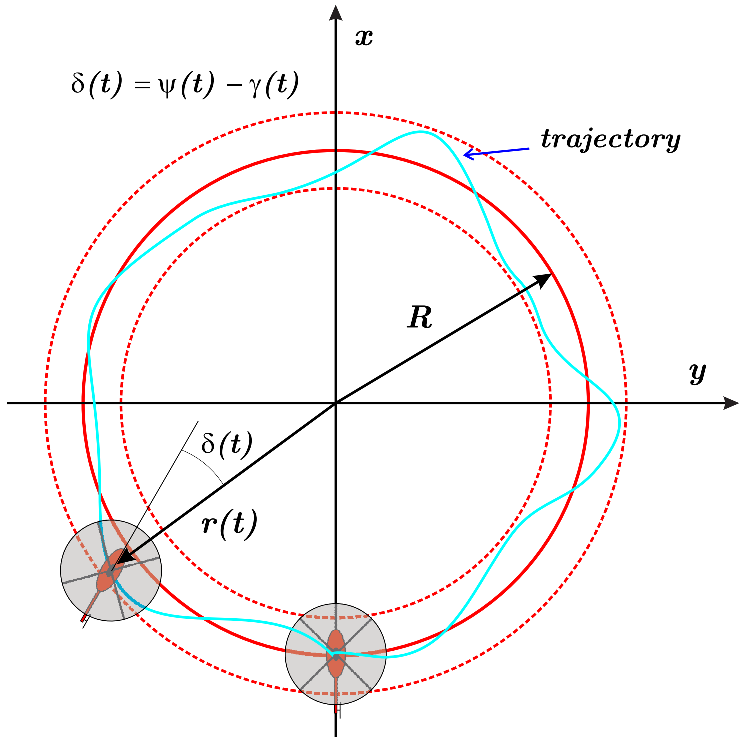

Fig. 6: **Pirouette. Top view.**

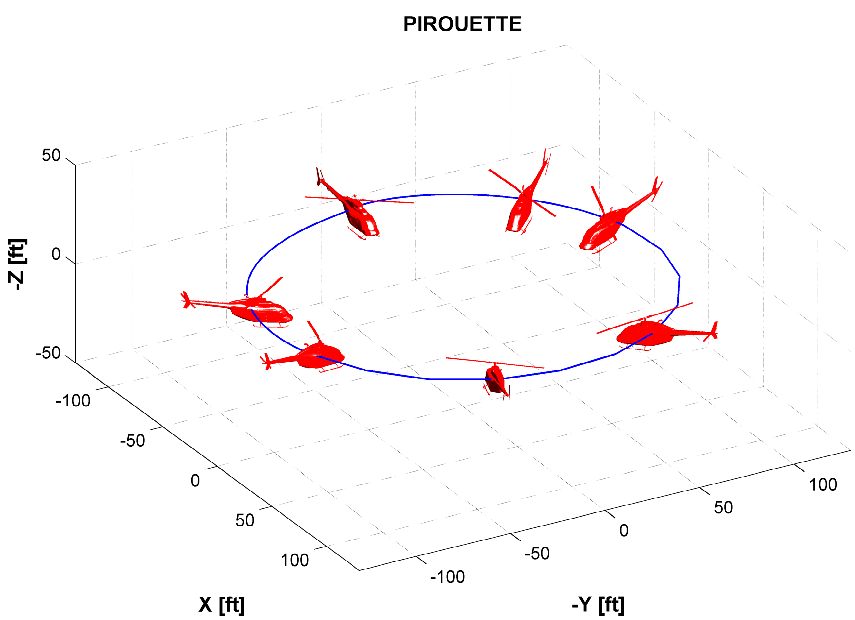

Fig. 7: **Pirouette. Snapshots.**

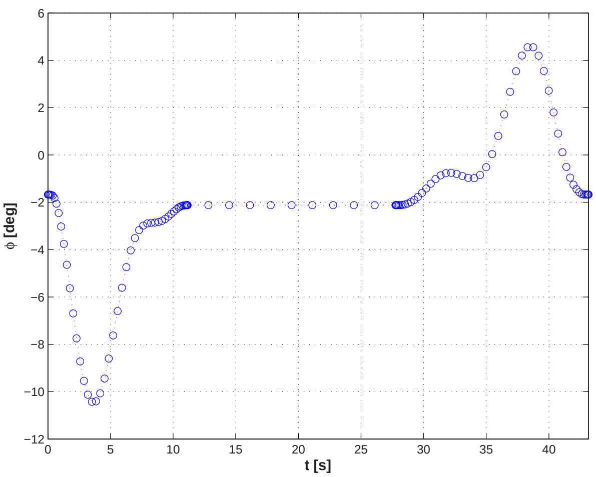

(a) *Roll.*

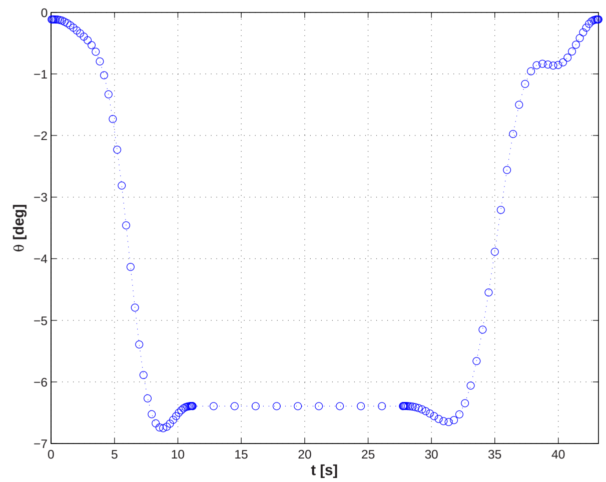

(b) *Pitch.*

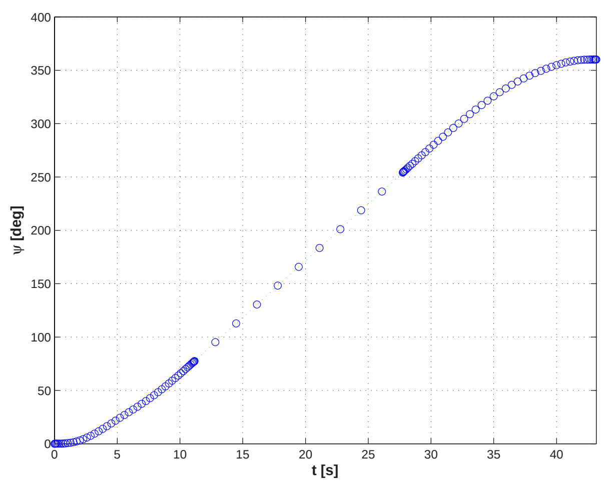

(c) *Yaw.*

Fig. 8: **Pirouette. Attitude angles.**

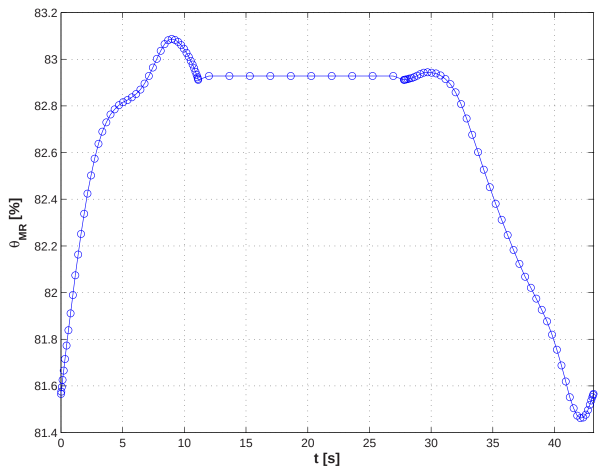

(a) *M/R Collective.*

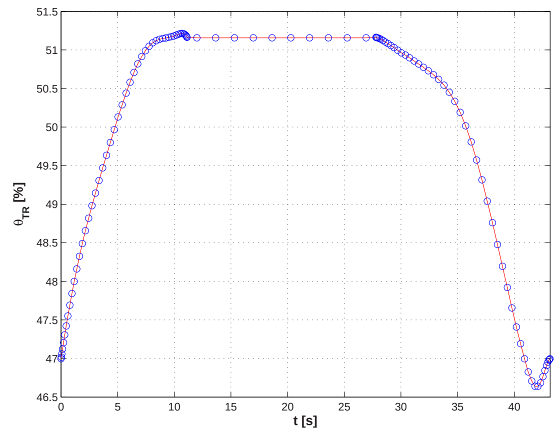

(b) *T/R Collective.*

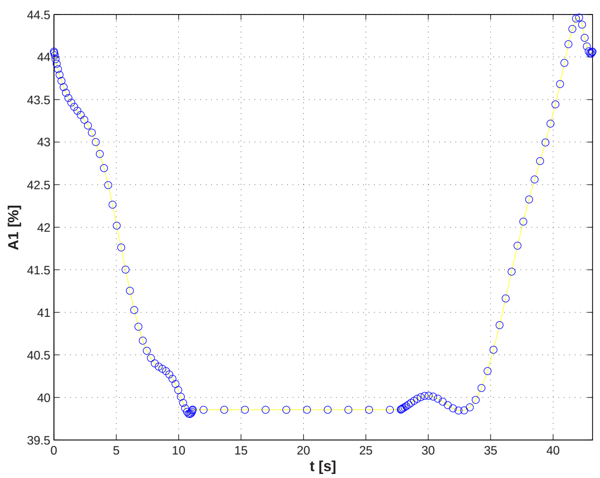

(c) *Lateral Cyclic.*

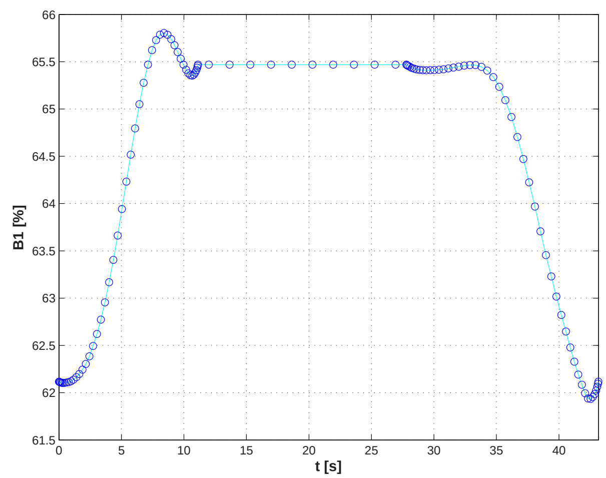

(d) *Longitudinal Cyclic.*

Fig. 9: **Pirouette. Controls.**

Furthermore, for the first/last transition we enforce the following equality constraints

$$\left[\frac{r(t_{0/N}) - R}{\Delta R}\right]^2 = 0, \tag{18a}$$

$$\left[\frac{\psi(t_{0/N}) - \gamma(t_{0/N})}{\Delta \psi}\right]^2 = 0. \tag{18b}$$

It should be noted that, for the first phase, the final position and heading angle are not imposed directly, but the constraints of Eqs. (18a) and (18b) require that at the end of the maneuver the vehicle is located in an unknown point along the reference circumference pointing its nose toward the center. The opposite approach is used for the last transition where the initial position is unknown, but constrained in an analogous way.

Figure 7 shows snapshots of the vehicle along its trajectory, while Figures 8 and 9 illustrate, respectively, the vehicle attitude in terms of its Euler angles and the optimal control inputs. The presence of the internal steady state condition, interposed between the two dynamic transitions, appears clearly from these plots. The maneuver duration is in compliance with the ADS-33 specification.

5.4 Slalom

As shown in Figure 10, for the Slalom maneuver the helicopter, starting from a stabilized Forward Flight and lined up with the centerline of the test course, is supposed to perform a series of turns and then recover the initial steady configuration. The test course is characterized by a series of obstacles at 500 ft intervals and alternatively located at ± 50 ft from the centerline; the maximum allowed lateral error is of 50 ft. The maneuver must be accomplished below the reference altitude of 100 ft. Furthermore, in this case the maneuver definition does not assign a maximum time, but rather specifies a minimum speed of at least 60 Knots throughout the slalom.

The simulation is characterized by a uniform grid of 100 steps and three obstacles. In order to introduce the presence of the obstacles in the simulation, the bounds of Table 1 are enforced for the ith pylon, where x_j and y_j represent the position (in the $x - y$ plane) at the jth node.

	Lower	**Upper**
x_{1+i20}	i 500 ft	i 500 ft
y_{1+i20}	$-35 + (-1)^i$ 75 ft	$+35 + (-1)^i$ 75 ft

Tab. 1: **Slalom. Position bounds for the obstacles.**

A specific lower bounds is imposed for the flight speed in order to guarantee the satisfaction of the lower value of 60 Knots imposed by the ADS-33 specification. The minimum time cost function is used again to reach a proper level of aggressiveness.

Figure 11 reports the computed trajectory, showing snapshots of the vehicle and the three obstacles. Figure 12 reports the optimal control time histories; the oscillating trend of the longitudinal and lateral cyclics is obviously related to the alternating left and right turns.

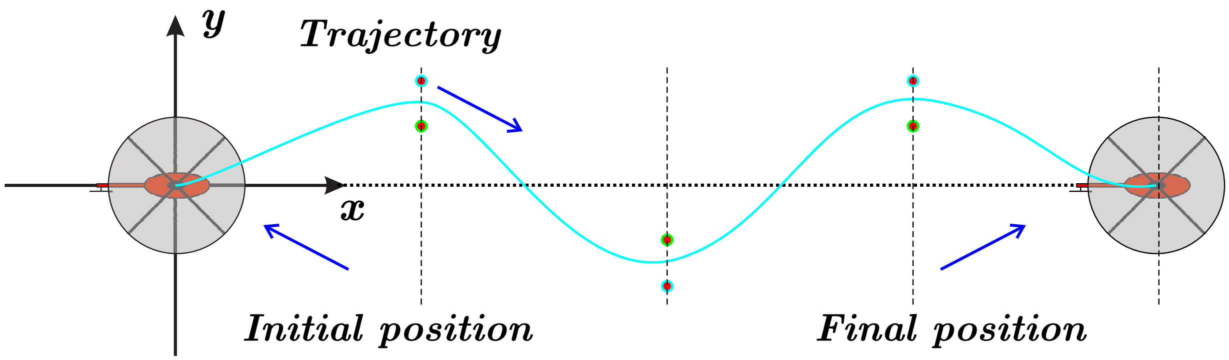

Fig. 10: **Slalom. Top view.**

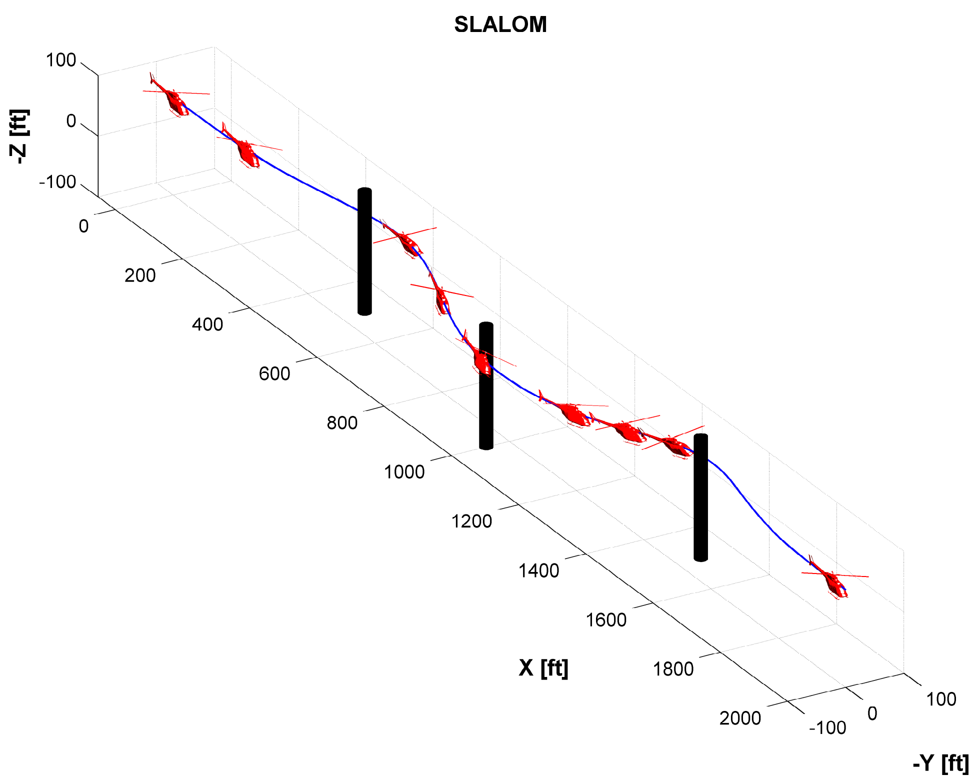

Fig. 11: **Slalom. Snapshots.**

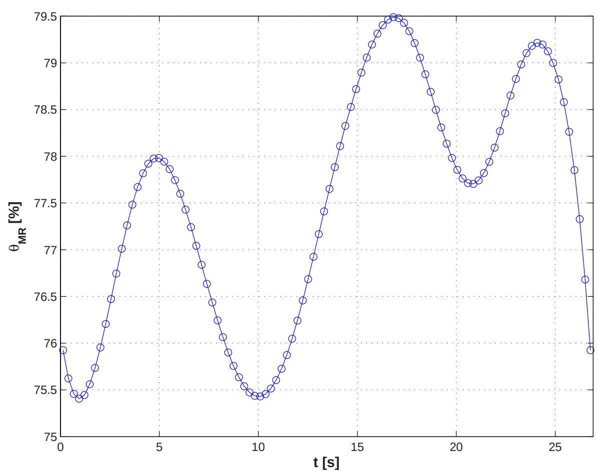

(a) *M/R Collective.*

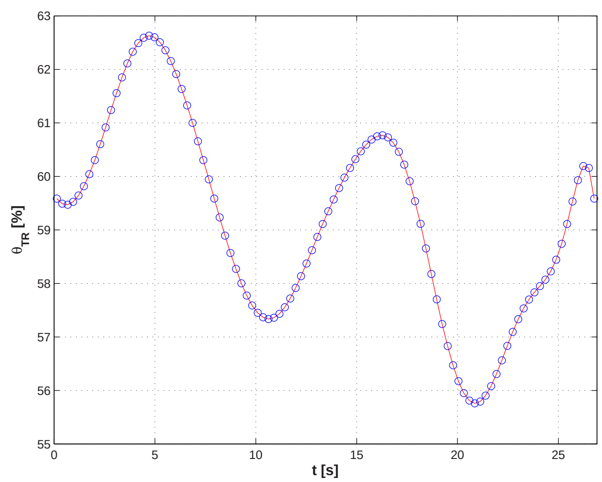

(b) *T/R Collective.*

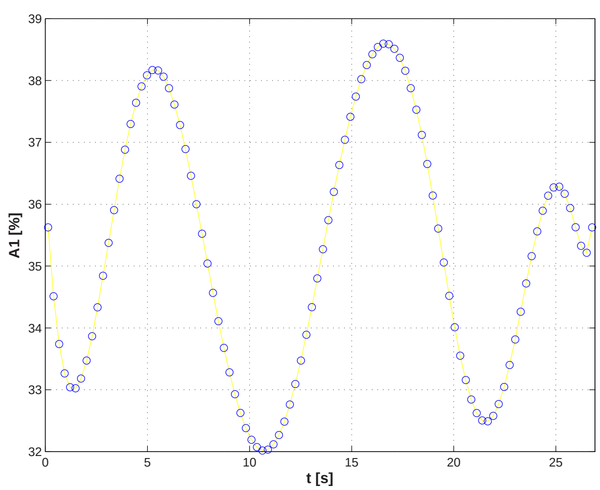

(c) *Lateral Cyclic.*

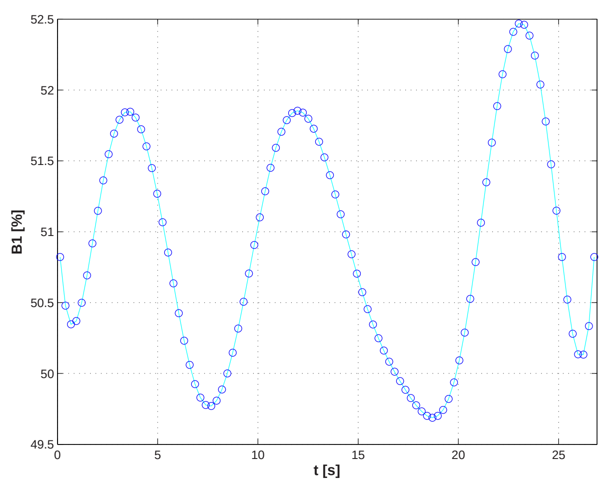

(d) *Longitudinal Cyclic.*

Fig. 12: **Slalom. Control inputs.**

6 CONCLUSIONS

In this document we have described a mathematical formulation for the analytical simulation of the ADS-33 MTEs. The problem is cast within the framework of optimal control theory. Using this approach, each maneuver is viewed as the solution of an appropriate constrained minimization problem; by specifying cost function and constraints, one gives a precise mathematical definition of the maneuver which is then computed by solving the resulting optimal control problem.

Path constraints reported in the ADS-33 specification can be easily introduced in the optimization process by position bounds, as shown for the Lateral Reposition and Slalom maneuvers, or using ad hoc single constraints, as in the case of the Pirouette. In order to be in compliance with the maximum time requirement, minimum time maneuvers were considered in this work. The resulting numerical method is typically quite robust since the two-point boundary value treatment of the problem can cope naturally with unstable systems such as helicopters; furthermore, the method is not very sensitive to the initial guess, especially if suitable boot-strapping procedures from crude meshes are used [9]. Using the proposed approach, we have compiled a complete library of MTE simulations, of which we have reported some representative examples in the present paper.

Future research for MTEs simulation will address the development of an alternative formulation which allows one to avoid the maneuver aggressiveness tuning phase, so as to be able to evaluate directly the maximum performance for a given vehicle. A further future effort will be related to the use of more sophisticated flight mechanics models. Typically, as the model complexity grows, the time step length must accordingly be reduced so that fast dynamic scales in the solution can be accurately captured. Using the Direct Transcription approach, the NLP problem dimension increases with the number of time steps, which in turn increases the computational cost. In this case, a better approach is to solve the problem by using the Multiple Shooting method, also available in the TOP code [11].

Acknowledgements

The present research is supported by AgustaWestland. The development of the interface with FLIGHTLAB was conducted at the AgustaWestland Flight-Mechanics office in Cascina Costa (VA-ITALY) and the results presented in this paper were obtained using AgustaWestland licenses. The contribution of Marco Cicalè, AgustaWestland flight mechanics manager, who has approved and verified the development of this research activity, is gratefully acknowledged.

References

[1] *Handling Qualities Requirements for Military Rotorcraft*, Aeronautical Design Standard, U.S. Army Aviation and Missile Command, Aviation Engineering Directorate, Rept. ADS-33E-PRF, Redstone Arsenal, AL, 2000.

[2] Johnson, W. *CAMRAD/JA: A Comprehensive Analytical Model of Rotorcraft Aerodynamics and Dynamics, Volume I: Theory Manual*, Johnson Aeronautics, 1988.

[3] BRITE-EURAM, 2000, RESPECT — Rotorcraft Efficient and Safe Procedures for Critical Trajectories.

[4] Advanced Rotorcraft Technology, Inc., 1685 Plymouth Street, Suite 250, Mountain View, CA 94043, http://www.flightlab.com.

[5] Howlett, J.J. *UH-60A Black Hawk Engineering Simulation Program: Volume I - Mathematical Model*, NASA Contractor Report 166309, National Aeronautics and Space Administration, Ames Research Center, Moffett Field, California, USA, 1981.

[6] *Advisory Circular 29-2C, Certification of Transport Category Rotorcraft*, Federal Aviation Administration, Department of Transportation, 1999.

[7] Okuno, Y. and Kawachi, K. Optimal Takeoff Procedures for a Transport Category Tiltrotor, *Journal of Aircraft*, May-June 1993, **30**, (3), pp 291–292.

[8] Carlson, E.B. and Zhao, Y.J. Optimal Short Takeoff of Tiltrotor Aircraft in One Engine Failure, *Journal of Aircraft*, March-April 2002, **39**, (2), pp 280–289.

[9] Bottasso, C.L., Croce, A., Leonello, D. and Riviello, L. Optimization of Critical Trajectories for Rotorcraft Vehicles, *Journal of the American Helicopter Society*, 2005, **50**, pp 165–177.

[10] Bottasso, C.L., Croce, A., Leonello, D. and Riviello, L. Rotorcraft Trajectory Optimization with Realizability Considerations, *Journal of Aerospace Engineering*, July 2005, **18**, (3), pp 146–155.

[11] Bottasso, C.L. Solution Procedures for Maneuvering Multibody Dynamics Problems for Vehicle Models of Varying Complexity, *Multibody Dynamics. Computational Methods and Applications*, Bottasso, C.L., Ed., Computational Methods in Applied Sciences, Springer-Verlag, Dordrecht, The Netherlands, 2008.

[12] Bottasso, C.L., Chang, C.S., Croce, A., Leonello, D. and Riviello, L. Adaptive Planning and Tracking of Trajectories for the Simulation of Maneuvers with Multibody Models, *Computer Methods in Applied Mechanics and Engineering*, Special Issue on Computational Multibody Dynamics, October 2006, **195**, (50-51), pp 7052–7072.

[13] Bottasso, C.L., Croce, A. and Leonello, D. Neural-Augmented Planning and Tracking Pilots for Maneuvering Multibody Dynamics, *Multibody Dynamics. Computational Methods and Applications*, García Orden, J.C., Goicolea, J.M. and Cuadrado, J., Eds., Computational Methods in Applied Sciences, ISBN 1-4020-5683-4, Springer-Verlag, Dordrecht, The Netherlands, 2007.

[14] Frazzoli, E. *Robust Hybrid Control for Autonomous Vehicle Motion Planning*, Ph.D. Thesis, Department of Aeronautics and Astronautics, Massachusetts Institute of Technology, Cambridge, MA, USA, 2001.

[15] Bauchau, O.A., Bottasso, C.L. and Nikishkov, Y.G. Modeling Rotorcraft Dynamics with Finite Element Multibody Procedures, *Mathematics and Computer Modeling*, May 2001, **33**, (10), pp 1113–1137.

[16] Geradin, M. and Cardona, A. *Flexible Multibody Dynamics, a Finite Element Approach*, John Wiley & Sons, New York, 2000.

[17] Bottasso, C.L. and Croce, A. Optimal Control of Multibody Systems using an Energy Preserving Direct Transcription Method, *Multibody System Dynamics*, August 2004, **12**, (1), pp 17–45.

[18] Bryson, A.E. and Ho, Y.C. *Applied Optimal Control*, Wiley, New York, 1975.

[19] Betts, J.T., *Practical Methods for Optimal Control using Non-Linear Programming*, SIAM, Philadelphia, 2001.

[20] Gill, P.E., Murray, W. and Wright, M.H. *Practical Optimization*, Academic Press, London and New York, 1981.

[21] Barclay, A., Gill, P.E. and Rosen, J.B. SQP Methods and Their Application to Numerical Optimal Control, Report NA 97–3, Department of Mathematics, University of California, San Diego, CA, 1997.

[22] Hull, D.G. Conversion of Optimal Control Problems into Parameter Optimization Problems, *Journal of Guidance, Control and Dynamics*, January, 1997, **20**, (1), pp 57–60.

[23] Griewank, A., Juedes, D., Mitev, H., Utke, J., Vogel, O. and Walther, A. ADOL-C: A Package for the Automatic Differentiation of Algorithms Written in C/C++, ACM TOMS, June 1996, **22**, (2), pp 131–167.